Chemical Engineering Journal 169 (2011) 231–238

Contents lists available at ScienceDirect

Chemical Engineering Journal

journal homepage: www.elsevier.com/locate/cej

Synthesis and characterization of Mg–Fe layer double hydroxides and its application on adsorption of Orange G from aqueous solution

N. Benselka-Hadj Abdelkader[a], A. Bentouami[b,c,*], Z. Derriche[a], N. Bettahar[a], L.-C. de Ménorval[d]

[a] Laboratoire de physico-chimique des matériaux – catalyse et environnement, USTO, BP 1505, 31000 El – M'Naouar, Oran, Algérie
[b] Département de chimie, Faculté des sciences, Université des Science et de la technologie d'Oran – USTO, BP 1505, 31000 El – M'Naouar, Oran, Algérie
[c] Laboratoire de Valorisation des matériaux, Université de Mostaganem, BP 227, Mostaganem, Algeria
[d] ICG–AIME–UMR 5253, Université Montpellier 2, Place Eugène Bataillon CC 1502, 34095 Montpellier Cedex 05, France

ARTICLE INFO

Article history:
Received 26 December 2010
Received in revised form 2 March 2011
Accepted 7 March 2011

Keywords:
Mg–Fe LDH
Adsorption
Pollutants
Acidic dye
Orange G

ABSTRACT

Layered double hydroxide (LDH) with hydrotalcite-like structure containing Mg(II) and Fe(III) in the layers and its calcined form were prepared at different Mg/Fe molar ration by co-precipitation method at fixed pH = 10 and followed by calcination at 500 °C (denoted CLDH). The obtained materials were characterized by powder X-ray diffraction (PXRD), FT-IR spectroscopy, and TGA. The prepared LDH and CLDH were used for Orange G (Acid Orange 10) dye removal from aqueous solutions. Batch studies were carried out to address various experimental parameters such as contact time, pH, sorbent dose and temperature. The sorption kinetics data fitted the pseudo-second order model. The isotherms were established and the parameters calculated. The sorption data fitted the Langmuir model with good values of the correlation coefficient. The sorption capacity of CLDH was found to be almost independent on initial pH of solution in the range 3–13 and approximately 5 times higher than that of LDH.

1. Introduction

Colour is the most apparent indicator of water pollution. The release of coloured wastes into receiving streams not merely affects the aesthetic nature but also interferes with transmission of sunlight into streams and therefore reduces photosynthetic activity [1]. Dyes can be classified as anionic (direct, acid and reactive dyes), cationic (basic dyes) and non-ionic (disperse dyes) [2]. Acid dyes are generally water soluble and are used for nylon, wool, silk, modified acrylics and also to some extent for paper, leather, inkjet printing, food and cosmetics. The principal chemical classes of these dyes are azo, anthraquinon, triphenylmethane, azine, xanthese, nitro and nitroso [3]. Orange G (Acid Orange 10) belongs to the acidic dye classes. In the USA Acid Orange 10 was used as a drug and cosmetic colorant until October 1966. According to the US National Toxicology program [4], Acid Orange 10 showed genotoxicity for Swiss Albino mice [5] and might be dangerous for humans as well [6]. Wastewaters offer great resistance for biodegradation due to presence of these heat and light stable dyes. Due to their low biodegradability, dyes are generally removed from aqueous solutions by sorption process using activated carbon [7–11]. The cost of this process led to several studies on alternative removal methods by use of less expensive natural materials and waste by-products such as sludge, perlite, rice husk, sawdust, bentonite, organophilic bentonites and layered double hydroxides [12–19].

Layered double hydroxides (LDHs), which are referred to anionic clays in comparison with cationic clays and also as hydrotalcite-like compounds (HT) are an important class of ionic lamellar solids. Layered double hydroxides (LDHs) with the general formula $[M^{2+}_{1-x}M^{3+}_{x}\ (OH)_2\ (A^{n-})_{x/n}]\cdot yH_2O$, have received considerable attention in recent years because of their potential applications such as ion exchangers, catalysts or catalyst supports, sorbents and antacids [20–23]. The structure of these solids is derived from a brucite structure in which trivalent cations partially substitute divalent ones. This substitution gives rise to positively charged layers balanced with interlayer anions; water molecules also exist in the inter-lamellar region [24,25]. The divalent (Mg^{2+}, Zn^{2+}, Cu^{2+}, etc.) and trivalent (Al^{3+}, Cr^{3+}, Fe^{3+}) cations occupy the center of $[M^{2+}/M^{3+}](OH)_6$ octahedral units and A^{n-} is an inorganic or organic anion. The calcination of (LDH) at 500 °C transforms them into mixed oxides (CLDH) which give the layered double hydroxide after rehydratation in the presence of the desired anion. This phenomenon is known as memory effect [26]. Due to their memory effect property, CLDH are suitable for sorption of anionic species.

From the survey of the literature, no information for the Orange G removal by uncalcined and calcined Mg–Fe–CO_3 layer double hydroxide is available. Therefore, the main objects of this present

* Corresponding author at: University of Sciences and Technolgy of Oran, Department of Chemistry, BP 1505, El M'Naouar, Oran, Algeria. Tel.: +213 771 90 61 44; fax: +213 41 56 03 62.
E-mail addresses: bentouami@gmail.com, a-bentouami@univ-usto.dz (A. Bentouami).

1385-8947/$ – see front matter © 2011 Elsevier B.V. All rights reserved.
doi:10.1016/j.cej.2011.03.019

work are: (i) the preparation and characterization of uncalcined and calcined Mg–Fe–CO_3 layer double hydroxide, (ii) the study of the feasibility of the obtained materials on Orange G adsorption, (iii) the determination of the various parameters affecting sorption and (iv) the study of the memory effect by X-ray diffraction of calcined Mg–Fe–CO_3 on its sorption of Orange G and carbonates anions.

2. Experimental

2.1. Starting materials

2.1.1. Hydrotalcite and calcined hydrotalcite

Mg–Fe–CO_3 (LDH), with various Mg/Fe molar ratios of 2–5 were prepared by co-precipitation at a fixed pH = 10, following the method described by Reichle [27]. A mixed solution of $MgCl_2$ $6H_2O$ (from 0.2 to 0.5 mol) and 0.1 mol of $FeCl_3$ $6H_2O$ in 100 ml of distilled water was added drop wise under vigorous stirring to 100 ml of an aqueous solution containing 0.2 mol of Na_2CO_3 and 0.1 mol of NaOH. During the co-precipitation process, the pH was maintained at a constant value equal to 10 by addition of 3 M NaOH solution. The suspension was stirred during 24 h at 80 °C for maturation and then centrifuged. The obtained material was washed with distilled water until obtaining a Cl^- free LDH ($AgNO_3$ test), dried during 24 h at 105 °C, ground in an agate mortar and 250 μm sieved. A fraction of the obtained material was calcined at 500 °C during 8 h. The obtained solid was designated as CLDH.

2.1.2. Sorbate

Orange G (Acid Orange 10) (purity ≥99%), a mono azoic and acid dye, is a synthetic dye provided by Across Organics and was used as received. Synthetic test dye solution was prepared by dissolving accurately a known amount of dye (1 g L^{-1}) in distilled water and subsequently diluting required concentrations.

2.1.3. Characterization of the prepared materials

Powder X-ray diffraction data were collected with monochromatic Cu Kα radiation (λ = 1.540589 Å) using a PHILIPS X'Pert MPD diffractometer. FT-IR spectra of LDH and CLDH (KBr disc samples) were recorded on a NICOLET Avatar 330 FT-IR spectrophotometer in the region of 400–4000 cm^{-1}. Thermogravimetric analyses (TGA) were performed with a Netzsch TGA 409 PC thermo balance with a heating rate of 20 °C/min from 25 to 900 °C.

2.2. Study of Orange G removal with LDH and CLDH

2.2.1. Kinetic study

Kinetic studies were conducted to find out the equilibrium time and the kinetic models of Orange G sorption by LDH and CLDH. In this study, the solid/solution (LDH or CLDH) ratio was 1 g L^{-1} and the initial concentration of Orange G was 200 mg L^{-1}. Suspensions were stirred for different time interval (5 min to 48 h) at room temperature and then centrifuged. The dye concentration in the supernatants was measured by visible spectrophotometer on SAFAS (Monaco 2000) UV–vis spectrophotometer at 480 nm. The adsorbed amounts were determined from the difference between the initial and final concentrations.

2.2.2. Sorption isotherms

The sorption isotherms were established using LDH and CLDH suspensions in Orange G solution (solid/solution ratio = 1 g L^{-1}) in a range from 50 to 800 mg L^{-1}. The suspensions were stirred during equilibrium times then centrifuged. The dye equilibrium concentration in the supernatants was determined by visible spectrophotometer at 480 nm.

The quantity of dye adsorbed at equilibrium was calculated by the following expression:

$$q_e = \frac{(C_0 - C_e)V}{m} \quad (1)$$

where m is the mass of sorbent (g), V is the volume of the solution (L), C_0 is the initial concentration of sorbate (mg L^{-1}), C_e is the equilibrium sorbate concentration (mg L^{-1}) and q_e is the quantity of sorbate adsorbed at equilibrium (mg of Orange G per g of sorbent)

2.2.3. Effect of the temperature

This effect was studied on suspensions of LDH and CLDH in a solid/solution ratio equals to 1 g L^{-1} in 300 and 500 mg L^{-1} of dye solution with LDH and CLDH, respectively. The suspensions were stirred at three constant temperatures (278, 298 and 323 K) during equilibrium time. The supernatants were separated by centrifugation and the equilibrium concentrations were determined as above.

2.2.4. Effect of LDH and CLDH dose

This effect was studied on suspension of LDH or CLDH in 300 or 500 mg L^{-1} of Orange G solution by varying solid/solution ratio from 0.1 to 1.8 g L^{-1} at natural pH of the dye (5.4). The suspensions were stirred during equilibrium times then centrifuged. The dye equilibrium concentration in the supernatants was determined as above.

2.2.5. Effect of initial pH

This effect was studied on suspensions of CLDH in 500 mg L^{-1} of Orange G dye solution (solid/solution ratio = 1.4 g L^{-1}). The initial pH of dye solution was adjusted to values in the range from 3 to 13 by the addition of 0.1 M NaOH or 0.1 M HCl solutions. The suspensions were stirred during the equilibrium time at room temperature, and then centrifuged. The dye concentration was determined as above.

2.2.6. Reconstruction by rehydration process (memory effect)

The rehydration process (reconstruction) of the layered structure was carried out with samples thermally decomposed at 500 °C. An amount of 50 mg of samples was suspended in 50 mL of Na_2CO_3 (0.5 mol L^{-1}) or of Orange G dye (500 mg L^{-1}) solution and stirred for 24 h at room temperature. The rehydration products were separated by centrifugation, washed several times with distilled water, dried at 105 °C over night then characterized by XRD.

3. Results and discussion

3.1. Characterizations of materials

The powder X-ray diffraction pattern of LDH with different Mg/Fe molar ratios (Fig. 1a) shows peaks at 7.7 Å (d_{003}), 3.84 Å (d_{006}), 2.64 Å (d_{012}), 1.55 Å (d_{110}) and 1.52 Å (d_{113}), which is similar to those reported by several authors [26–29]. By analyzing the X-ray diffractograms we obtained that cell parameters are a = 3.10 Å and c = 23.1 Å for LDH sample which are in good agreement with previous reports [26–30]. The influence of Mg/Fe molar ratios was apparent, it can be see from XRD (Fig. 1a) that with Mg/Fe molar ratio equals 3, the good cristalinity and higher hydrotalcite content in sample were obtained.

The diffractogram pattern of CLDH (hydrotalcite calcined) (Fig. 1b) shows peaks at 2θ = 43.06° and 62.48° which are corresponding to MgO, and at 2θ = 30.2°, 35.5°, 43.06°, 57.2° and 62.5° which can be attributed to the $MgFe_2O_4$ (magnesioferrite) spinel structure (JCPDS 17-0465) those peaks have been observed by Ferreira et al. [26] and Zhang et al. [31].

The FT-IR spectra of LDH with different Mg/Fe molar ratios shown in Fig. 2 are typical of layer double hydroxides and agree well

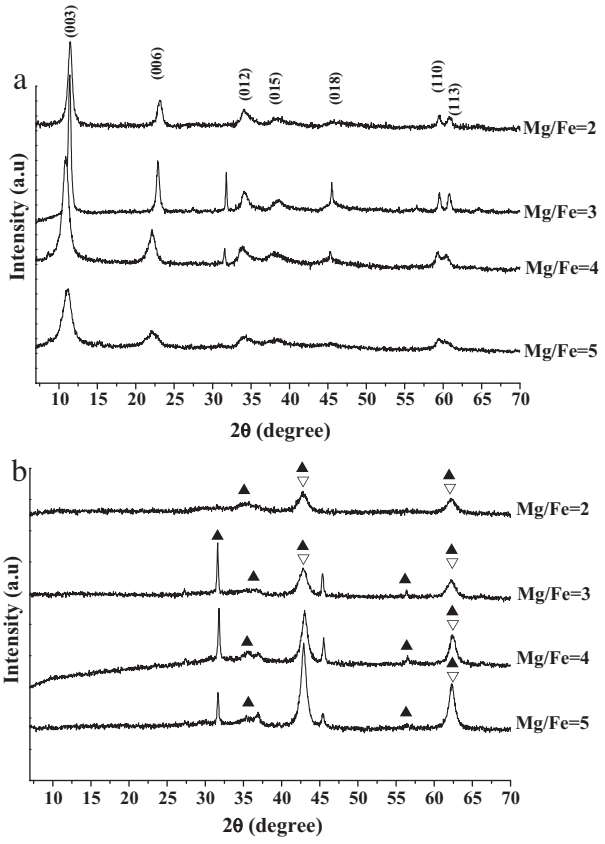

Fig. 1. XRD patterns of uncalcined MgFe-LDH with various Mg/Fe ratios (a) and samples calcined at 773 K (b); (▲) $MgFe_2O_4$; (▽) MgO.

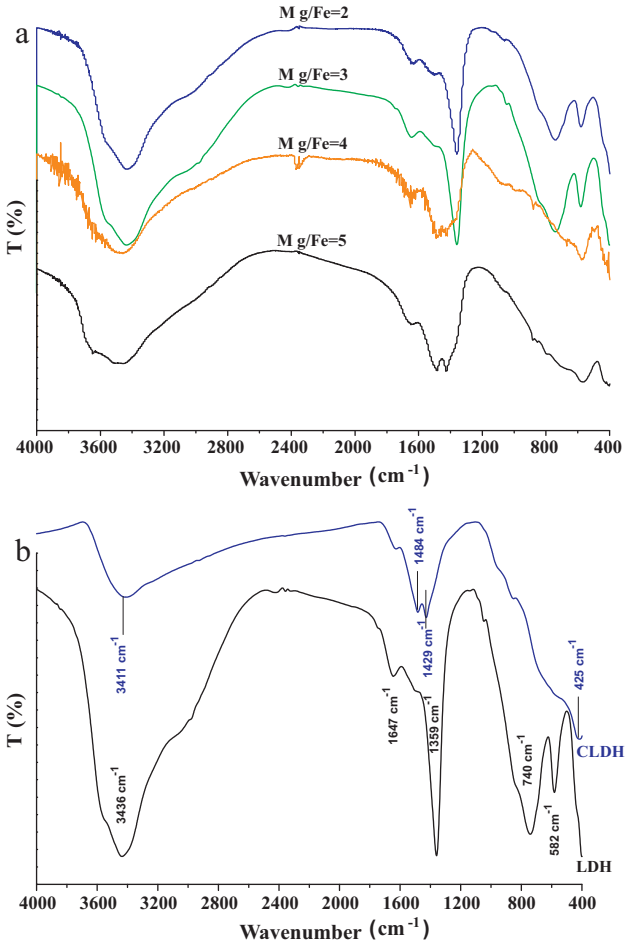

Fig. 2. FT-IR spectra of uncalcined (LDH) with different Mg/Fe ratios (a) and LDH and calcined (CLDH) Mg–Fe–CO_3 with Mg/Fe = 3 (b).

with the typical results obtained by Ferreira et al. [26]. The broad band observed at 3436 cm^{-1} is attributed to the interlayer water molecules, this band become weaker and is shifted at 3411 cm^{-1} when hydrotalcite is calcined. The weak band at 1647 cm^{-1} is due to the bending vibration (deformation mode of HOH (δ_{H-O-H})) of interlayer water molecules in LDH [25–29]. The strong band at 1359 cm^{-1} is due to the mode ν_3 of the interlayer carbonate species as reported in the literature [26,30]. The bands in the range of 500–750 cm^{-1} are attributed to metal–oxygen–metal stretching [25–30].

The TGA plot for LDH sample (Fig. 3) shows three distinct weight losses in the temperature ranges 50–200, 200–460 and 460–750 °C. The weight loss in the first step (50–200 °C) was about 13% which is a common characteristic of hydrotalcites related to the loss of physisorbed and interlayer water. The second weight loss, which occurs between 200 and 460 °C, was due to the first step of dehydroxylation and the removal of carbonate ions from the interlayer and represents a mass loss of 21%. Over this temperature range, the hydrotalcite undergo decarbonatation and dehydroxylation reactions and produce metal oxides. In the third, final mass loss (about 5%) that occurs further than 460 °C can due to continuous dehydroxylation and decarbonatation and formation of oxide metals as MgO, which are detected in X-ray diffractogram of CLDH (hydrotalcite calcined at 500 °C), and probably $MgFe_2O_4$ as reported by Ferreira et al. [26].

3.2. Study of Orange G removal with LDH and CLDH

All this study was established with LDH and CLDH prepared by co-precipitation with Mg/Fe molar ration equals 3.

3.2.1. Contact time effect on Orange G adsorption

Plots of removed amounts of Orange G per gram of solid (q_t) versus contact time presented in Fig. 4 shows that the sorption equilibrium of Orange G was reached after 12 and 9 h on LDH and CLDH, respectively. Zhu et al. reported that equilibrium time required for Brilliant Blue R (BBR) sorption by calcined LDH was less than 12 h, whereas, BBR sorption by uncalcined LDH was longer than 20 h [18]. The difference between equilibrium time obtained with LDH and CLDH can be explained that dye adsorption on LDH may occur

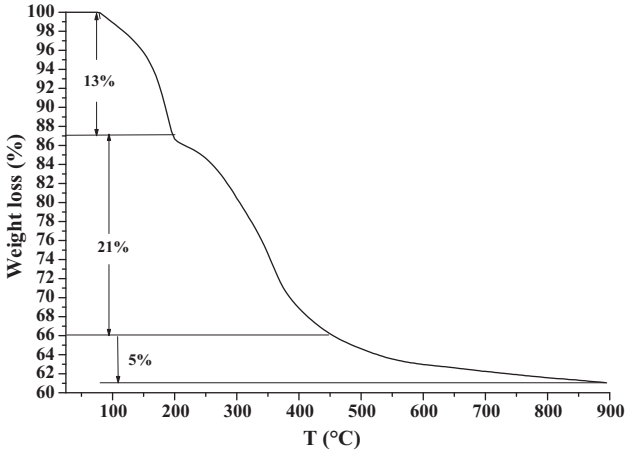

Fig. 3. TGA plot of uncalcined Mg–Fe–CO_3.

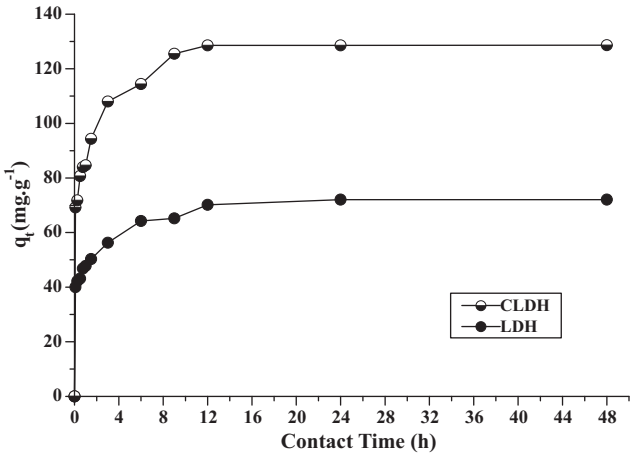

Fig. 4. Effect of contact time on Orange G adsorption on LDH and CLDH, $C_0 = 200\ mg\ L^{-1}$

via exchange mechanism, but on CLDH, it occurs probably by both surface and ion exchange phenomena by reconstruction (memory effect). Furthermore, for the same initial dye concentration, the adsorbed amount is higher on CLDH than on LDH.

From these preliminary results and for the following sorption study, the contact time of 12 h and 9 h were selected to ensure the sorption equilibrium with LDH and CLDH, respectively.

3.2.2. Kinetic modelling

The sorption kinetics is an important aspect of the pollutant removal process control. The Lagergren pseudo-first-order model [32], the Ho and McKay pseudo-second-order model [33–37], and the Weber and Morris intra-particle diffusion model [38] are the most frequently used in the literature to predict the involved mechanism in the sorption process.

The Lagergren pseudo-first-order model is expressed by the following equation [32]:

$$\frac{dq}{dt} = k_1(q_e - q_t) \quad (2)$$

where q_t and q_e (mg g^{-1}) are respectively the amounts of adsorbed dye at time t and at equilibrium and k_1 (min^{-1} or h^{-1}) is the first-order rate constant. Integration of Eq. (2) gives the following expression:

$$Ln(q_e - q_t) = Ln(q_e) - k_1 t \quad (3)$$

Eq. (3) shows a linear relationship between Ln($q_e - q_t$) and t. Linear regression calculation allows to obtain the values of the rate constant k_1 and the equilibrium adsorption capacity q_e. These parameters were calculated for the adsorption of Orange G on LDH and CLDH. The results are plotted in Fig. 5 and the calculated parameters reported in Table 1. According to correlation coefficient (R^2) values which are lower than 0.93 for both materials, we can infer that the experimental results did not fit the pseudo-first-order model. Moreover, large differences between experimental and calculated values of the equilibrium adsorption capacity are observed for both LDH and CLDH (Table 1).

A pseudo-second-order model may also describe the kinetic sorption of Orange G on LDH and CLDH. According to Ho and McKay [33–37], the differential equation for this model is

$$\frac{dq_t}{dt} = k_2(q_e - q_t)^2 \quad (4)$$

where, q_t and q_e (mg g^{-1}) are respectively the amounts of adsorbed dye at time t and at equilibrium and k_2 (h^{-1} (mg/g)$^{-1}$) is the pseudo-second-order rate constant.

Table 1
Kinetic parameters for Orange G adsorption by LDH and CLDH.

Sorbent	Experimental	Pseudo-first-order model			Pseudo-second-order model				Intra-particle diffusion model		
	q_e, exp (mg g^{-1})	k_1 (h^{-1})	q_e, cal (mg g^{-1})	R^2	k_2 (h^{-1} (mg/g)$^{-1}$)	q_e, cal (mg g^{-1})	h (mg g^{-1}/h)	R^2	k_{id} (mg g^{-1} h$^{-0.5}$)	C (mg g^{-1})	R^2
LDH	72.08	0.2278	35.23	0.9126	0.0269	72.8	142.6	0.9996	9.658	37.90	0.9714
CLDH	128.60	0.3977	66.99	0.9277	0.0199	129.9	335.8	0.9998	21.045	65.00	0.9825

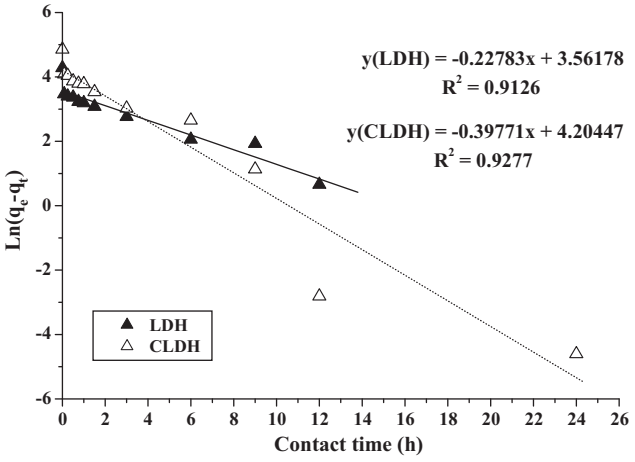

Fig. 5. Pseudo-first-order plots for Orange G adsorption on LDH and CLDH.

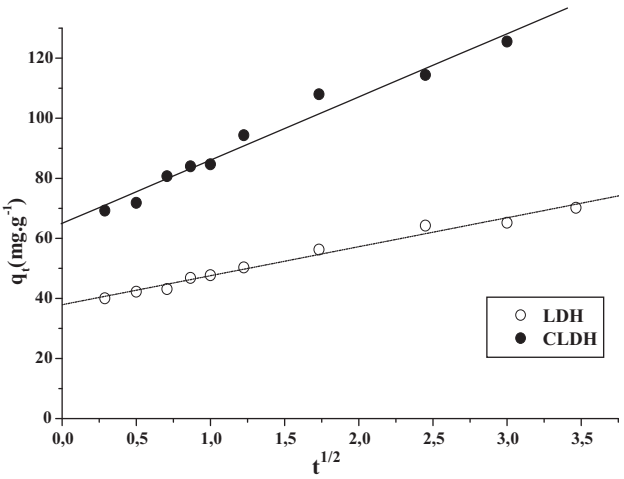

Fig. 7. Weber and Morris plots of Orange G adsorption on LDH and CLDH.

The integration of Eq. (4) and its linearization gives the following expression:

$$\frac{t}{q_t} = \frac{1}{k_2 q_e^2} + \frac{1}{q_e} t \tag{5}$$

If the initial sorption rate is:

$$h = k_2 q_e^2 \tag{6}$$

Then Eq. (5) becomes:

$$\frac{t}{q_t} = \frac{1}{h} + \frac{1}{q_e} t \tag{7}$$

The plots of t/q_t versus t (Fig. 6) are straight lines where slopes and intercepts are $1/q_e$ and $1/k_2 q_e^2$, respectively. The values of the rate constant k_2, of the equilibrium sorption capacity q_e and initial sorption rate are calculated from these parameters. The calculated k_2, q_e and h values and the corresponding linear regression correlation coefficient R^2 values for both LDH and CLDH are reported in Table 1. Very good correlation is observed between experimental data and the pseudo-second-order kinetic model with correlation coefficient values close to unity ($R^2 > 0.999$), which showed that the Orange G uptake process by both LDH and CLDH followed the pseudo-second-order model. Besides, low differences between experimental and calculated values of Orange G equilibrium sorption capacity were observed and are less than 1%.

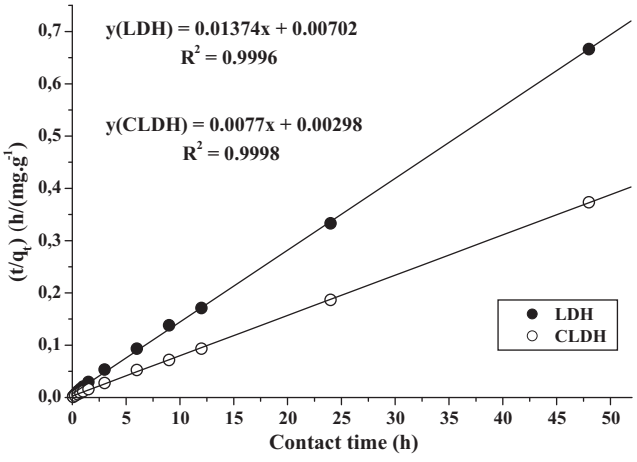

Fig. 6. Pseudo-second-order plots for Orange G adsorption on LDH and CLDH.

The intra-particle diffusion model knows as the Weber and Morris model [38] is expressed by the following equation:

$$q_t = k_{id} t^{0.5} + C \tag{8}$$

where, q_t is the amount of Orange G adsorbed at time t, C the intercept and k_{id} ($mg\,g^{-1}\,h^{-0.5}$) is the intra particle diffusion rate constant. This latter is determined from the linear plot (Fig. 7) of q_t versus $t^{0.5}$, and it is usually used to compare the mass transfer rates. If the plot does not pass through the origin, this is indicative of some degree of boundary layer control and intra particle diffusion is not the sole rate limiting step. The intercept values are 37.90 and 65.00 $mg\,g^{-1}$ for LDH and CLDH, respectively (Table 1), which indicates that pore diffusion is not rate limiting step [37–40].

3.2.3. Sorption isotherm

The equilibrium sorption experimental data of Orange G dye by CLDH and LDH were analysed using the most frequently used Freundlich and Langmuir isotherm models.

The empirical Freundlich model which is known to be adequate for low concentrations is expressed by the following equation [41]:

$$q_e = K_F C_e^{1/n} \tag{9}$$

where q_e is the equilibrium concentration of solute per gram of adsorbent ($mg\,g^{-1}$), C_e is the equilibrium aqueous concentration of the solute ($mg\,L^{-1}$), K_F and n are Freundlich constants which are related to adsorption and intensity of adsorption.

Eq. (9) can be linearized in its logarithmic form, which allows the determination of Freundlich constants as below:

$$\log q_e = \frac{1}{n} \log C_e + \log K_F \tag{10}$$

The Langmuir isotherms model is described by the following equation [42]:

$$q_e = \frac{Q_{max} K_L C_e}{1 + K_L C_e} \tag{11}$$

where q_e (mg/g) is the amount of dye removed per gram of sorbent, Q_{max} ($mg\,g^{-1}$) is the maximum sorption capacity, C_e ($mg\,L^{-1}$) is the equilibrium dye concentration and K_L ($L\,mg^{-1}$) is the Langmuir constant related to adsorption energy.

The linear form of Langmuir equation can be expressed as below:

$$\frac{C_e}{q_e} = \frac{C_e}{Q_{max}} + \frac{1}{Q_{max} K_L} \tag{12}$$

The values of K_F, $1/n$, Q_{max}, K_L and the correlation coefficients for Langmuir and Freundlich models are given in Table 2. It can

Table 2
Freundlich and Langmuir isotherm constants for Orange G dye adsorption on LDH and CLDH.

Sorbent	Freundlich model			Langmuir model		
	n	K_F	R^2	K_L (L g^{-1})	Q_{max} (mg g^{-1})	R^2
LDH	4.63	21.4	0.8291	0.074	76.4	0.9982
CLDH	2.72	41.7	0.9504	0.023	378.8	0.9959

be seen from Table 2 that the correlations coefficient R^2 values for Langmuir model are higher than those of Freundlich model. Thus we can deduce that adsorption isotherms for both materials are better represented by Langmuir model than the Freundlich model. Furthermore, the maximum sorption capacity of CLDH was found approximately 5 times higher (378.8 mg g^{-1}) than that of LDH (76.4 mg g^{-1}). Mall et al. have obtained 18.8 mg of Orange G adsorbed per gram of bagasse fly ash [43].

3.2.4. Effect of the temperature

The study of the temperature effect on Orange G adsorption on LDH and CLDH enabled us to determine the thermodynamic parameters (ΔG°, ΔH° and ΔS°) of these reactions by using the following equation:

$$\ln K_d = \frac{\Delta S^\circ}{R} - \frac{\Delta H^\circ}{RT} \quad (13)$$

where R is ideal gas constant, T is the temperature (K), K_d (L g^{-1}) is the distribution coefficient which is calculated with the following expression:

$$K_d = \frac{q_e}{C_e} \quad (14)$$

The plot of ln(K_d) versus 1000/T for both LDH and CLDH gives a straight line, the slope and the intercept correspond to $\Delta H^\circ/R$ and $\Delta S^\circ/R$, respectively.

The thermodynamic parameters calculated from the values of the slopes and intercepts are reported in Table 3. Generally, the change in adsorption enthalpy for physisorption is in the range of −20 to 40 kJ/mol, but for chemisorption is between −400 and −80 kJ/mol [44]. Positive values of ΔH° indicate that adsorption of Orange G on both LDH and CLDH is an endothermic process and physical in nature. Furthermore, negative values of ΔG° indicate that the Orange G adsorption is spontaneous on both materials. The positive values of ΔS° indicate an increasing randomness at solid-solution interface during adsorption process.

3.2.5. Effect of LDH and CLDH dose

The adsorption of Orange G on CLDH as function of sorbent dose is shown in Fig. 8. The Orange G amount adsorbed by both LDH and CLDH increase with increasing sorbent dose until 1.4 g L^{-1}, from this dose the quantities of dye adsorbed on both materials were still unchanged. This may be explained by the good dispersion of materials particles on Orange G solutions, where the adsorbed and exchanged sites of materials were probably more open.

3.2.6. Effect of initial pH

Fig. 9 shows the plots of Orange G amount adsorbed versus initial pH solution ranging from 3 to 13. From the Fig. 9, it was observed

Table 3
Thermodynamic parameters for the adsorption of Orange G on LDH and CLDH.

	ΔS° (J/mol K)	ΔH° (kJ/mol)	ΔG° (kJ/mol)		
			273 K	298 K	323 K
LDH	157.13	31.81	−11.87	−15.01	−18.94
CLDH	132.56	21.28	−15.57	−18.22	−21.53

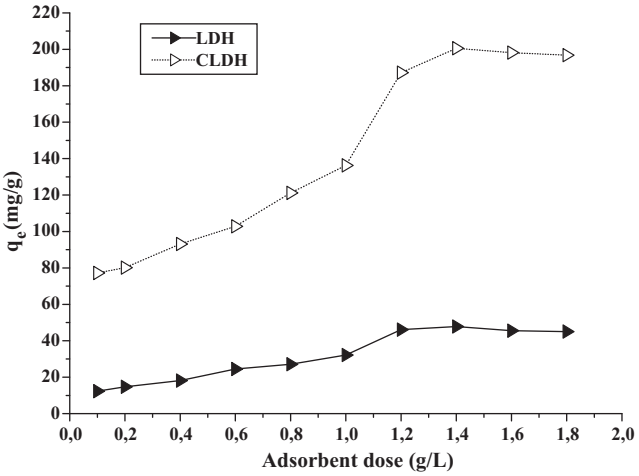

Fig. 8. Effect of adsorbent dose on Orange G adsorption.

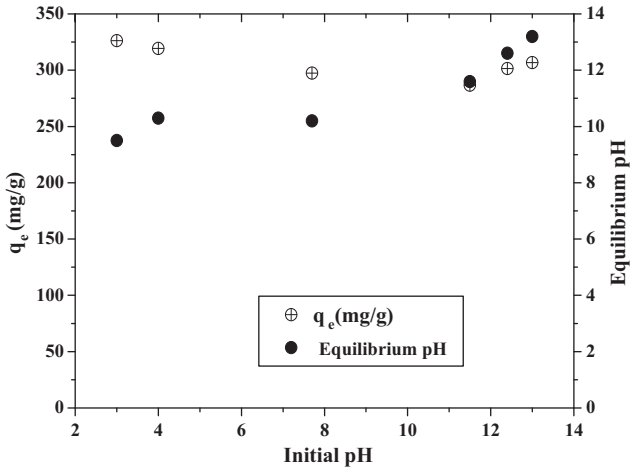

Fig. 9. Initial pH effect on Orange G adsorption on CLDH.

that the initial pH did not affect the adsorption of Orange G on CLDH, but the final pH increases with increasing initial pH. Similar observation was reported in the literature with almost similar adsorbents [18,25].

3.2.7. Reconstruction by rehydration process (memory effect)

The anionic layered material can be reconstructed by rehydration by immersion of the calcined solid in water containing anionic species [45]. Fig. 10 shows the X-ray diffraction pattern of the original CLDH without rehydration, with rehydration on carbonates solution (0.5 mol L^{-1}) and with rehydration on Orange G solution (500 mg L^{-1}). Fig. 10 shows characteristic peaks of the same LDH as the starting phase with a loss in their relative intensity reflecting a slight fall in the crystallinity of the material. The rehydration of the mixed oxides obtained after calcination at 773 K of the starting material (LDH) gives in the presence of carbontae anions an hydrotalcite phase with good cristallinity than that in the presence of Orange G dye (Fig. 10c), the same observations was reported by Ferreira et al. [26]. Nevertheless, the intensity of the peaks had decreased compared with the starting LDH because of some reduction in crystallinity following the calcination and rehydration. However, no evident change in the interlayer spacing was observed (d_{003} = 8.0 Å for calcined LDH rehydrated in the presence of Orange G dye and 7.7 Å for starting LDH) indicating that the Orange G was adsorbed onto the surface of the LDH rather than intercalated between the

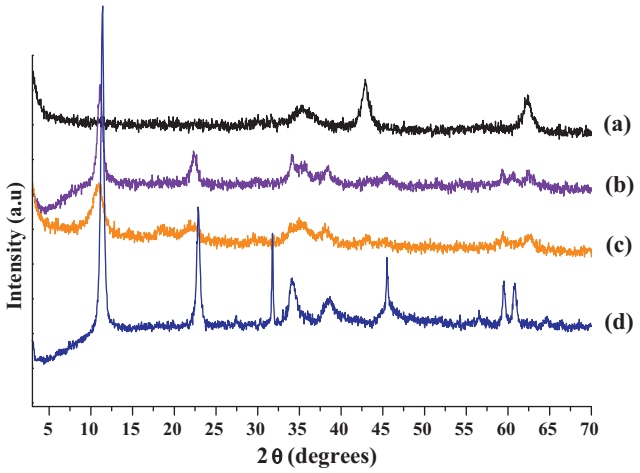

Fig. 10. Powder X-ray diffractogramm of: (a) original calcined (CLDH) Mg–Fe–CO_3, (b) rehydration on carbonates solution, (c) rehydration on Orange G solution and (d) starting uncalcined (LDH) Mg–Fe–CO_3.

interlayer. Similar observations have been cited by Yuan et al. [46].

4. Conclusion

In this work, an uncalcined and calcined Mg–Fe–CO_3 layer double hydroxides were prepared. The obtained materials were characterized and used for an acidic dye (Orange G) removal from aqueous solutions. The study of Orange G adsorption on both LDH and CLDH indicate that:

(1) The kinetic results fit the pseudo-second-order model with correlation coefficient values nearly to unity for the two materials with initial sorption rate on CLDH higher than that on LDH. The higher intercept values indicate that pore diffusion is not rate limiting step of the sorption process.
(2) The Orange G sorption follows the Langmuir model with correlation coefficient higher than 0.99 for the two materials. The Orange G sorption capacity of CLDH is approximately 5 times higher than that of LDH and other. The sorption capacity of CLDH was found to be independent on pH in the range from 3 to 13.
(3) The values of the thermodynamic parameters obtained indicated that the Orange G sorption was spontaneous and endothermic in nature.

Consequently, it has been demonstrated the efficiency of the uncalcined and calcined Mg–Fe–CO_3 layer double hydroxides on Orange G adsorption, for this reason those two materials could be used to decolorize anionic dyes as Orange G from wastewater. Therefore, the work is in progress to determine the mechanism of Orange G adsorption on LDH and CLDH and also to improve the dye removal rate.

References

[1] C. Namasivaya, R. Radhika, S. Suba, Uptake of dyes by a promising locally available agricultural solid waste: coir pith, Waste Manage. 21 (2001) 381–387.
[2] G. Mishra, M. Tripathy, A critical review of the treatment for decolorization of textile effluent, Colourage 40 (1993) 35–38.
[3] V.K. Gupta, Suhas, Application of low-cost adsorbents for dye removal—a review, J. Environ. Manage. 90 (2009) 2313–2342.
[4] US National Toxicology Program, 2007. http://ntp-server.niehs.nih.gov.
[5] A.K. Giri, A. Mukherjee, G. Talukder, A. Shrama, In vivo cytogenetic studies on mice exposed to Orange G, a food colourant, Toxicol. Lett. 44 (1988) 253–261.
[6] N. Jović-Jovičić, A. Milutinović-Nikolić, P. Banković, Z. Mojović, M. Žunić, I. Gržetić, D. Jovanović, Organo-inorganic bentonite for simultaneous adsorption of Acid Orange 10 and lead ions, Appl. Clay Sci. 47 (2010) 452–456.
[7] O. Gulnaz, A. Kaya, F. Matyar, B. Arikan, Sorption of basic dyes from aqueous solution by activated sludge, J. Hazard. Mater. 108 (2004) 183–188.
[8] W.T. Tsai, C.Y. Chang, M.C. Lin, S.F. Chien, H.F. Sun, M.F. Hsieh, Adsorption of acid dye onto activated carbons prepared from agricultural waste ZnCl2 activation, Chemosphere 45 (2001) 51–58.
[9] P.C.C. Faria, J.J. Morfao, M.F.R. Pereira, Adsorption of anionic and cationic dyes on activated carbons with different surface chemistries, Water Res. 38 (2004) 2043–2052.
[10] K. Nakagawa, A. Namba, S.R. Mukai, H. Tamon, P. Ariyadejwanich, W. Tanthapanichakoon, Adsorption of phenol and reactive dye from aqueous solution on activated carbons derived from solid wastes, Water Res. 38 (2004) 1791–1798.
[11] V. Meshko, L. Markovska, M. Mincheva, A.F. Rodrigues, Adsorption of basic dyes on granular activated carbon and natural zeolite, Water Res. 35 (2001) 3357–3366.
[12] M. Bagane, S. Guiza, Elimination d'un colorant des effluents de l'industrie textile par adsorption, Ann. Chim. Sci. Mater. 25 (2000) 615–626.
[13] M. Otero, F. Rozada, L.F. Calvo, A.I. Garcia, A. Moran, Elimination of organic water pollutants using adsorbents obtained from sewage sludge, Dyes Pigments 57 (2003) 55–65.
[14] O. Demirbas, M. Alkan, M. Dogan, The removal of Victoria blue from aqueous solution by adsorption on a low-cost material, Adsorption 8 (2002) 341–349.
[15] P.K. Malik, Use of activated carbons prepared from sawdust and rice-husk for adsorption of acid dyes: a case study of acid yellow 36, Dyes Pigments 56 (2003) 239–249.
[16] D.K. Singh, B. Srivastava, Basic dyes removal from wastewater by adsorption on rice husk carbon, Indian J. Chem. Technol. 8 (2001) 133–139.
[17] S.H. Lee, D.I. Song, Y.W. Jeon, An investigation of the adsorption of organic dyes onto organo-montmorillonite, Environ. Technol. 22 (2001) 247–254.
[18] M.X. Zhu, Y.P. Li, M. Xie, H.Z. Xin, Sorption of an anionic dye by uncalcined and calcined layered double hydroxides: a case study, J. Hazard. Mater. B120 (2005) 163–171.
[19] J. Orthman, H.Y. Zhu, G.Q. Lu, Use of anion clay hydrotalcite to remove coloured organics from aqueous solutions, Sep. Purif. Technol. 31 (2003) 53–59.
[20] I. Carpani, M. Berrettoni, B. Blaring, M. Giorgetti, E. Scavetta, D. Tonelli, Study on the intercalation of hexacyanoferrate(II) in a Ni–Al based hydrotalcite, Solid State Ionics 168 (2004) 167–175.
[21] P.A. Terry, Characterization of Cr ion exchange with hydrotalcite, Chemosphere 57 (2004) 541–546.
[22] A. Vaccari, Clays and catalysis: a promising future, Appl. Clay Sci. 14 (1999) 161–198.
[23] F. Malherbe, C. Depège, C. Forano, J.P. Besse, M.P. Atkins, B. Sharma, S.R. Wade, Alkoxylation reaction catalysed by layered double hydroxides, Appl. Clay Sci. 13 (1998) 451–466.
[24] F. Cavani, F. Trifiro, A. Vaccari, Hydrotalcite-type anionic clays: preparation, properties and application, Catal Today 11 (1991) 173–301.
[25] M. Bouraada, M. Lafjah, M.S. Ouali, L.-C. de Ménorval, Basic dye removal from aqueous solutions by dodecylsulfate- and dodecyl benzene sulfonate-intercalated hydrotalcite, J. Hazard. Mater. 153 (2008) 911–918.
[26] O.P. Ferreira, O.L. Alves, D.X. Gouveia, A.G. Souza Filho, J.A.C. de Paiva, J. Mendes Filho, Thermal decomposition and structural Reconstruction effect on Mg–Fe-based hydrotalcite compounds, J. Solid State Chem. 177 (2004) 3058–3069.
[27] W.T. Reichle, Synthesis of anionic clay minerals (mixed metal hydroxides, hydrotalcite), Solid State Ionics 22 (1986) 135–141.
[28] J.M. Fernandez, M.A. Ulibarri, F.M. Labajos, V. Rives, The effect of iron on the crystalline phases formed upon thermal decomposition of Mg–Al–Fe hydrotalcites, J. Mater. Chem. 8 (1998) 2507–2514.
[29] F. Kovanda, V. Balek, V. Dorniěák, P. Martinec, M. Mašláò, L. Bílková, D. Koloušek, I.M. Bountsewa, Thermal behaviour of synthetic pyroaurite-like anionic clay, J. Therm. Anal. Calorim. 71 (2003) 727–737.
[30] R. Trujillano, M.J. Holgado, J.L. González, V. Rives, Cu–Al–Fe layered double hydroxides with CO_3^{2-} and anionic surfactants with different alkyl chains in the interlayer, Solid State Sci. 7 (2005) 931–935.
[31] H. Zhang, R. Qi, D.G. Evans, X. Due, Synthesis and characterization of a novel-scale magnetic solid base catalyst involving a layered double hydroxide supported on a ferrite core, J. Solid State Chem. 177 (2004) 772–780.
[32] S. Lagergren, About the theory of so-called adsorption of soluble substances, Handlingar 24 (1898) 1–39.
[33] Y.S. Ho, G. McKay, Kinetic model for lead (II) sorption on to peat, Adsorpt. Sci. Technol. 16 (1998) 243–255.
[34] Y.S. Ho, G. McKay, Pseudo-second order model for sorption processes, Process Biochem. 34 (1999) 451–465.
[35] Y.S. Ho, G. McKay, The Kinetics of sorption of divalent metal ions onto sphagnum moss peat, Water Res. 34 (2000) 735–742.
[36] Y.S. Ho, G. McKay, Application of kinetic models to the sorption of copper (II) on to peat, Adsorpt. Sci. Technol. 20 (2002) 797–815.
[37] Y.S. Ho, Second-order kinetic model for the sorption of cadmium onto tree fern: a comparison of linear and non-linear methods, Water Res. 40 (2006) 119–125.
[38] W.J. Weber, J.C. Morris, Kinetics of adsorption on carbon from solution, J. Sanit. Eng. Div. Am. Soc. Civ. Eng. 89 (1963) 31–59.
[39] I.D. Mall, V.C. Srivastava, N.K. Agarwal, Removal of Orange-G and methyl violet dyes by adsorption onto bagasse fly ash-kinetic study and equilibrium isotherm analyses, Dyes Pigments 69 (2006) 210–223.

[40] M. Mana, M.S. Ouali, L.C. de Menorval, Removal of basic dyes from aqueous solutions with a treated spent bleaching earth, J. Colloid Interface Sci. 307 (2007) 9–16.
[41] H.M.F. Freundlich, Uber die adsorption in lusungen, Z. Phy. Chem. 57 (1906) 385–470.
[42] I. Langmuir, The adsorption of gases on plane surfaces of glass, mica and platinium, J. Am. Chem. Soc. 40 (1918) 1361–1403.
[43] I.D. Mall, V.C. Srivastava, N.K. Agarwal, Removal of Orange-G and methyl violet dyes by adsorption onto bagasse fly ash—kinetic study and equilibrium isotherm analyses, Dyes Pigmemts 69 (2006) 210–223.
[44] L. Lian, L. Guo, C. Guo, Adsorption of Congo red from aqueous solutions onto Ca-bentonite, J. Hazard. Mater. 161 (2009) 126–131.
[45] V. Rives, M. Angeles Ulibarri, Layered double hydroxides (LDH) intercalated with metal coordination compounds and oxometalates, Coord. Chem. Rev. 181 (1999) 61–120.
[46] S. Yuan, Y. Li, Q. Zhang, H. Wang, ZnO nanorods decorated calcined Mg–Al layered double hydroxides as photocatalysts with a high adsorptive capacity, Colloids Surf. A 348 (2009) 76–81.